International Journal of Engineering

Journal Homepage: www.ije.ir

Aeolian Vibrations of Transmission Line Conductors with More than One Damper

A. Rezaei*, M. H. Sadeghi

Mechanical Engineering Department, University of Tabriz, Tabriz, Iran

PAPER INFO

Paper history:
Received 23 June 2015
Received in revised form 01 September 2015
Accepted 03 September 2015

Keywords:
Aeolian Vibration
Transmission Line
Stock–bridge Damper
Energy Dissipation

ABSTRACT

To reduce the damages of aeolian vibration of conductors to the power transmission networks, the most common method is installation of Stock-bridge dampers. Estimation of the damper's dissipated energy is an important factor in determining the number and location of installation of these types of vibration absorbers. This estimation is strongly dependent upon the assumed mode shape of the conductor vibration. The results of current study show that the available methods do not provide an accurate answer for energy dissipation of a conductor with more than one damper. This paper provides a comprehensive method for calculating the mode shapes and dissipated energy in which the effects of travelling wave, amplitude and phase variations, boundary conditions as well as the influence of the number, position, and impedance of the dampers on the mode shape are taken into account. Moreover, the frequency bands of high-amplitude vibration potential can be identified without the need to extract the vibration amplitude.

doi: *10.5829/idosi.ije.2015.28.10a.16*

1. INTRODUCTION

Overhead transmission line vibrations cause severe damage to electrical transmission lines. Aeolian vibrations are the most common type of conductor vibrations which occur in high frequency and small amplitude that give rise to the fatigue failure of the conductor strands. These vibrations occur at laminar flow (or low turbulence) winds with low velocities (1 to 7 m/s) and their peak to peak amplitude reaches to the conductor diameter [1-4]. Wind velocity component perpendicular to the conductor leads to the formation of Von-Karman vortex, giving rise to an alternative vertical force and excitation of the conductor in the vertical plane [5]. Due to the conductor small internal damping, particularly at low frequencies, the use of external dampers is necessary to reduce the conductor vibration amplitude, for extending the conductor's service life [6]. Accordingly different types of dampers are used for energy absorption in the distribution and transmission lines [7]. The application of Stock-bridge damper (Figure 1) is the most common way to achieve this goal [1]. This type of damper not only dissipates energy due to its messenger cable's strand slippage, but also acts as a dynamic-vibration absorber.

Predicting the vibration behavior of a conductor with different number of dampers is essential for estimating the damper performance and conductor service life. The dynamic analysis of conductor and study of its vibration modes and its effects starts with electric power transmission network developments. The empirical study of the factors affecting the aeolian vibration and failure of electrical line conductors due to fatigue, started about a century ago [8]. However, the theoretical modeling of this phenomenon began in nearly half a century ago [9]. Theoretical research to simulate conductor vibration along with the experimental test to evaluate vibration state and predict transmission lines fatigue life has been continued up until now [10-12].

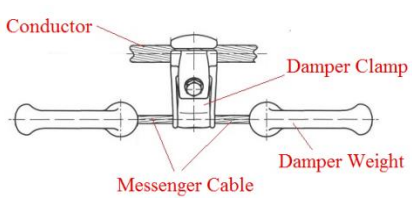

Figure 1. Stock-bridge damper [13]

*Corresponding Author's Email: *a.rezaei@tabrizu.ac.ir* (A. Rezaei)

Please cite this article as: A. Rezaei, M.H. Sadeghi, Aeolian Vibrations of Transmission Line Conductors with More than One Damper, International Journal of Engineering (IJE), TRANSACTIONS A: Basics Vol. 28, No. 10 (October 2015) 1515-1524

In the practical arena, the energy balance method (EBM) is employed to determine the maximum amplitude of the conductor vibration [4, 12, 14-19]. Steady-state vibration amplitude obtained by this method depends heavily upon the amount of estimated energy dissipation which itself is calculated based on assumptions made about mode shapes of vibration. In the classical procedure of EBM, the dissipated energy estimation is done by the assumption of a standing harmonic wave in the entire span [20]. This method is very simple, but it does not reflect the effects of damper impedance and the travelling wave. To overcome these shortcomings, the response of the conductor vibration is considered as a superposition of two harmonic traveling waves which propagate in opposite directions on the semi-infinite conductor (Hagedorn Method) [15]. For a conductor with single damper, this method leads to satisfactory results and is accepted as a practical method and has been used up until now [17, 18]. The method is also extended to conductors with several dampers [19]. However, as shown in the present study, the use of this method for conductors with more than one damper do not yield accurate outcome and giving rise to the damper dissipated power do not considerably change with the increase in the number of dampers. The shortcomings of the given approach originate from the adoption of unrealistic assumptions, as the Hagedorn method is based upon the assumption of semi-infinite conductor which considers the propagation of wave in the two sides of the span independently. Furthermore, the fixed boundary conditions of the clamped ends are not taken into account in the extraction of the vibration mode shapes. In the Hagedorn method, the amplitude and phase of the travelling waves are assumed to be constant along the conductor. Moreover, due to the assumption of infinite conductor length, eigenvalue problem is not solved, so that each frequency is considered as a natural frequency with a simple sinusoidal wave as the mode shape of the sub-span vibrations.

The review of the related literature shows that there is no comprehensive approach for calculating the dissipated energy of the conductors with more than one damper. To overcome this deficiency, the present study provides a new method that not only considers the effects of the number, location and impedance of the damper on the vibration mode shapes and energy dissipation, but also considers the effects of boundary conditions (finite length of the conductor), the travelling wave and phase-amplitude changes along the span. Comparison between the results of the conventional and proposed methods reveals that considering the aforementioned aspects have significant impact on the accuracy of the response.

In this study, the effects of the travelling wave, damper location, damper impedance and damping rate on deformation of mode shape, energy dissipation and phase-amplitude changes are investigated, and the limits associated with the low and high damping rates are also identified. By determining the low damping areas in frequency domain, the identification of frequency bands with high potential of vibrations is facilitated without the need to calculate the vibration amplitude.

2. THE CONDUCTOR VIBRATION

In this section, a model of the steady-state vibration of a single conductor with Stock-bridge damper is described.

2. 1. Equation of Vibration Due to the high tension-to-weight ratio in transmission lines, the conductor in-plane vibration equation can be well approximated as [15-22]:

$$EI\,u^{IV} - T\,u'' + \rho\ddot{u} = F_w(x,t) + F_c(u,\dot{u},t) \quad (1)$$

in which EI is the bending stiffness (or flexural rigidity), T is the tensile force, ρ is the mass per unit length, $u(x,t)$ is the vertical displacement, F_w is the wind force (resulting from Karman vortex) and F_c is the conductor internal damping force. The dot sign represents the derivative with respect to time (t) and the prime symbol indicates the derivative with respect to the spatial coordinate (x).

The actual value of conductor bending stiffness is a function of the conductor curvature at any point, and therefore, depends on time and space [20]. The effect of variable bending stiffness has been investigated by some authors [23, 24]. Since the transmission lines are designed for the worst case scenario, the value of the bending stiffness is considered to be constant and is equal to its minimum limit [1, 20, 25].

However, due to dense frequency spectrum and occurrence of the lock-in phenomenon in the electric power transmission lines, steady wind at any speed will cause steady vibration of the conductor in resonance, i.e. the frequency and mode shape of the steady forced vibration of the conductor will always correspond to one of its natural frequencies and the related mode shape. Also, the bending stiffness and internal damping of the conductor has a little influence on determining the natural frequency and mode shape of the conductor [15-21, 25-27]. Therefore, the mode shapes of the conductor may be obtained from the following equation which is the taut string free vibration equation [15-21], and V_c refers to the wave propagation velocity along the string [28]:

$$\ddot{u} = V_c^{\,2}\,u'' \quad , \quad V_c^{\,2} = T/\rho \quad (2)$$

2. 2. The Dissipated Power Energy dissipation in the conductor has a number of different sources. The combination of all types of conductor damping is known as conductor self-damping [20, 21]. The dissipated power of the conductor is measured through the "power", "standing wave" and "decay" methods [29] and its mathematical relations are presented in different references [4, 15, 17, 26, 27, 29, 30]. In general, the dissipated power of the conductor is negligible compared with the one of damper [15-18].

Average power dissipation of the Stock-bridge damper (P_d) following the experimental measurement of damper impedance is calculated through Equation (3) in which τ refers to the time period of vibration.

$$P_d = \frac{1}{\tau}\int_0^{\tau} \text{real}(\bar{F}_d \cdot \bar{V}_d)\, dt = \frac{1}{\tau}\int_0^{\tau} \text{real}(Z_d \cdot (\bar{V}_d)^2)\, dt \quad (3)$$

(The subscript d is used for the quantities associated with the damper).

Since considering the rotational displacement of the damper clamp has not a discernible effect on energy dissipation [16, 26], the damper impedance is measured only in the translational displacement. Mechanical impedance of the damper is calculated according to IEC 61897 [31] following the experimental measurement of the exerted force on damper clamp and clamp vibration velocity:

$$\bar{F}_d = F_d\, e^{i(\omega t+\theta_F)} \quad , \quad \omega = 2\pi f$$
$$\bar{V}_d = V_d\, e^{i(\omega t+\theta_V)} \quad , \quad V_d = \omega A_d \quad (4)$$
$$\bar{Z}_d = \frac{\bar{F}_d}{\bar{V}_d} = Z_d\, e^{i(\omega t+\theta_z)}$$

In the above Equation, F_d is the amplitude of measured exerted force on damper at frequency ω, V_d is the damper velocity amplitude, $\theta_Z = \theta_F - \theta_V$ is the phase measured between the force and the velocity signal s and Z_d is the calculated damper impedance (at that specific frequency and velocity). Figures 2 and 3 show the setup of the Stock-bridge damper impedance test and output of the test, respectively, which is performed in the Vibration Research Laboratory, University of Tabriz. After determining the impedance, by Equation (4) and replacing it in Equation (3), the dissipated power of the damper is calculated by following equation (in terms of damper displacement amplitude):

$$P_d = \frac{1}{2} Z_d\, (\omega A_d)^2 \cos(\theta_z) \quad (5)$$

Since the vibration amplitude of the damper (A_d) in Equation (5) is calculated by the conductor vibration mode shape, the assumed mode shape for conductor can have a major effect on the accuracy of the obtained results for the damper dissipated power and conductor vibration amplitude. To put it differently, various assumptions about the form of the conductor vibration lead to different results in the estimation of the dissipated power of damper.

2. 3. Various Assumed Mode Shapes The simplest solution of Equation (2) is the sinusoidal standing wave. In this case, mode shape of the vibration is regarded as harmonic standing waves in entire span. Therefore, damper displacement amplitude is simply calculated as [1]:

$$A_d = A\sin(k\, x_d) \quad , \quad k = \frac{\omega}{V_c} \quad (6)$$

In this Equation, x_d is the distance of the damper installation point from the support and k is the wave number. The effect of travelling wave and damper impedance on mode shapes and phase-amplitude changes along the conductor are ignored. To overcome these shortcomings, the steady-state response of the conductor including a Stock-bridge damper is considered as the superposition of two travelling waves with the identical frequency that propagate in the opposite directions on the semi-infinite conductor [15-19]:

$$u(x,t) = G_1\sin(k(x+V_c t)) + G_2\cos(k(x+V_c t)) + H_1\sin(k(x-V_c t)) + H_2\cos(k(x-V_c t))$$
$$A_f = \sqrt{G_1^2+G_2^2} \quad , \quad A_b = \sqrt{H_1^2+H_2^2} \quad (7)$$

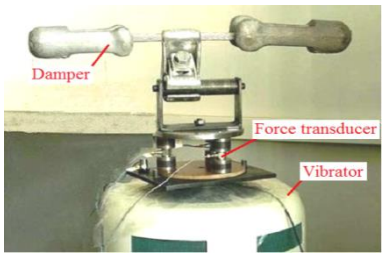

Figure 2. Connecting the Stock-bridge damper to vibrator with force sensors

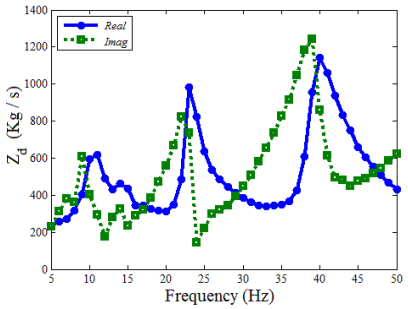

Figure 3. Experimental results for the impedance of Stock-bridge damper

The incoming wave amplitude towards the damper (A_f) and the reflected one (A_b), in general have different values, which are obtained by applying boundary conditions. Then the "absorption coefficient" (the ratio of damper absorbed energy to the emitted energy) is calculated as [4, 15-19]:

$$\alpha = \frac{\Delta P}{P_{in}} = \frac{(A_f)^2 - (A_b)^2}{(A_f)^2} = 1 - (\frac{A_b}{A_f})^2 \quad (8)$$

Also, dissipated power of the damper in terms of absorption coefficient and amplitude of the vibration (A) is obtained as [15-19]:

$$P_d = \frac{1}{4}\frac{T}{V_c}\omega^2 A^2 (\frac{\alpha}{2-\alpha}) \quad (9)$$

Absorption coefficient (α) has always a value in the range $0 \le \alpha \le 1$. Limit values of zero and one, respectively, represent the complete and zero absorption of the energy.

To calculate the energy dissipation in a conductor with more than one damper which is installed on both sides of the span, a generalized version of the above method is used [19]. Since the span length of power transmission lines reaches to hundreds of meters, and wind energy is transmitted from the middle of the span to the two sides, finite conductor is considered as two semi-infinite conductors in the above method [15-19].

Although the assumption of travelling wave with constant amplitude on the semi-infinite conductor leads to satisfactory results for a single damper conductor, this study shows that using this method is not valid for calculating the dissipated power of conductors with more than one damper. As the number of dampers increase, no significant change is seen in the energy dissipation obtained by this method. This result clearly contradicts with the reality and damper performance in energy dissipation. The cause of this apparent contradiction is revealed by a closer look at the effects of increased number of dampers on the energy dissipation. In the Hagedorn method, by using the amplitudes of backward and forward waves in the last sub-span, the absorption coefficient is calculated at the first step, and then energy dissipation is obtained by Equation (9) in terms of absorption coefficient. Based on this equation, increase in the number of dampers can only lead to more energy dissipation by increase in the absorption coefficient. On the other hand, the absorption coefficient for one or any number of dampers installed in the "appropriate place" is at most one. Therefore, an increase in the number of dampers cannot significantly affect the increase in the absorption coefficient. Based on obtained results, the absorption coefficients related to the installation of more than two dampers on a semi-infinite conductor, are identical, consequently energy dissipation does not change by installing three, four or five dampers on the conductor (Figure 4).

Such contradiction in the results using Hagedorn method originates from the adoption of unreal assumptions regarding the extraction of the absorption coefficient and the dissipated energy relations. On one hand, despite the sources of energy dissipation in the system, the phase-amplitude is considered to be constant in the entire span. On the other hand, to consider the travelling wave, the conductor is assumed to be infinite. By taking the infinite conductor for granted, the eigenvalue problem of the conductor vibration is not solved and each frequency is considered natural and the simple sinusoidal wave is regarded as the mode shape of the sub-span vibrations. The energy emitted from the middle of the span to the two ends of the conductor is assumed to be completely independent of each other as well [15].

3. THE PROPOSED METHOD

In the proposed method, an appropriate model is presented for vibration of the conductors with several dampers that can yield more accurate results for the conductor vibration response and damper dissipated energy. The following factors are considered in our new approach: travelling wave effect, finite length of the conductor (including boundary conditions), the effect of the number, location and impedance of the dampers as well as the influence of variation of the phase-amplitude with respect to time and spatial coordinates. In the proposed method, by taking into account the complex form of the general response of the conductor vibration equation, the eigenvalue problem of the conductor vibration is formed, following the solution which leads to the natural frequencies, the damping rates and complex mode shapes. Then the dissipated power of each damper is calculated individually. In the proposed method, no unreal constraint is imposed upon the problem.

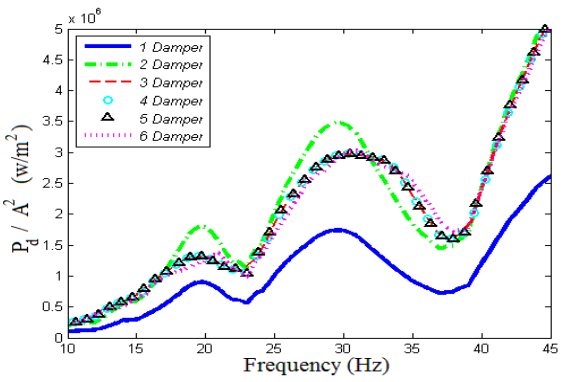

Figure 4. Change of relative dissipation power for a conductor with different number of dampers using the conventional assumption

To extract the general response for the finite length conductor vibration equation, the d'Alembert solution for the general solution of Equation (2) is considered as follows [32]:

$$u_1(x,t) = g_1(t + \frac{x}{V_c}) + g_2(t - \frac{x}{V_c}) \tag{10}$$

In this Equation, g_1 and g_2 are arbitrary functions that indicate the travelling waveform. Based on experimental observations, the arbitrary functions are assumed harmonic. Therefore, the following response will be given, which is the same as Equation (7):

$$u_2(x,t) = A_0 \sin(\omega(t + \frac{x}{V_c}) + \theta_1) + B_0 \sin(\omega(t - \frac{x}{V_c}) + \theta_2) \tag{11}$$

It can be noted that the above equation can be rewritten as follows:

$$u_2(x,t) = \text{real}(e^{st}(\bar{A}_0 e^{\gamma x} + \bar{B}_0 e^{-\gamma x}))$$
$$\bar{A}_0 = A_0 e^{i\theta_A} \ , \ \bar{B}_0 = B_0 e^{i\theta_B}$$
$$\gamma = \frac{x}{V_c} \ , \ s = i\omega \tag{12}$$

To reflect the effect of damping, the eigenvalue s instead of being a purely imaginary number, should be a complex number whose imaginary part is the vibration frequency and its real part is the damping rate. As a result, the response of conductor vibration equation takes the following form:

$$s = -\delta + i\omega \ , \ \zeta = \frac{\delta}{\sqrt{(\delta^2 + \omega^2)}} \tag{13}$$

$$u(x,t) = \text{real}(e^{st}(\bar{A}_0 e^{\gamma x} + \bar{B}_0 e^{-\gamma x})) = e^{-\delta t}\begin{pmatrix} A_0 e^{-\frac{\delta}{V_c}x} \sin(\omega(t + \frac{x}{V_c}) + \theta_A) + \\ B_0 e^{\frac{\delta}{V_c}x} \sin(\omega(t - \frac{x}{V_c}) + \theta_B) \end{pmatrix} \tag{14}$$

In the above Equation, δ and ζ are the damping rate and the dimensionless damping factor, respectively.

Also, for the aeolian vibration with small amplitude and slope, vertical component of conductor tension (q) is written as follows:

$$q = T \cdot \sin(\theta_u) \cong T \cdot \tan(\theta_u) = T \frac{du}{dx} \tag{15}$$

Therefore:

$$q(x,t) = \text{real}(\bar{q}(x,t)) \ , \ \bar{q}(x,t) = T \frac{d\bar{u}}{dx} \tag{16}$$

In general, a span with n_d dampers (Figure 5), has ($n_d + 1$) sub-spans and thus will have $2 \times (n_d + 1)$ complex unknowns -in addition to the s value- which are the complex amplitudes of sub-spans travelling waves. To extract these unknowns, we need the same number of complex equations that can be provided by the application of boundary condition at both ends of the span as well as the geometric and force conditions at each damper location:

$$\bar{u}(x_1 = 0 \ , \ t) = \bar{u}(x_{n_d+1} = l_{n_d+1} \ , \ t) = 0 \tag{17}$$

$$\begin{cases} (\bar{u}(x,t))_{x_p = l_p} = (\bar{u}(x_1,t))_{x_{p+1}=0} \\ (\bar{q})_{x_{p+1}=0} - (\bar{q})_{x_p = l_p} = \bar{F}_d \end{cases}$$
$$\bar{F}_d = \bar{Z}_d \cdot (\frac{d\bar{u}}{dx})_{x_p = 0} \ , \ p = 1,2,3,...,n_d \tag{18}$$

By applying the above constraints and solving the obtained eigenvalue problem, the sub-spans amplitudes ($\bar{A}_0, \bar{B}_0$) and the eigenvalues (s) i.e. the natural frequencies, damping rates and the eigenvectors (natural complex mode shapes) are obtained.

For a conductor without a damper, the above method leads to standing wave and completely imaginary eigenvalues. Namely, for damper-free conductor the new approach is adapted to the classic standing wave method. Therefore, there is no need for formation and solution of another eigenvalue problem, and the associated frequencies and mode shapes are obtained by:

$$s = \pm i\omega \ , \ \omega = n\frac{\pi V_c}{L} \ , \ n = 0, 1, 2, ...$$
$$u(x,t) = A \sin(kx) \times \sin(\omega t + \theta) \ , \ k = \frac{\omega}{V_c} \tag{19}$$

4. RESULTS AND DISCUSSION

In the present study a new method for calculating the conductor mode shapes and damper dissipated energy is proposed which takes into account the phase-amplitude changes with respect to the time along the span by assuming the eigenvalue in a complex form. This is in addition to considering the effect of traveling wave and damper impedance on the mode shapes.

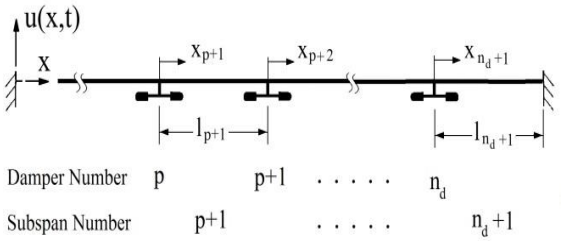

Figure 5. A conductor with more than one damper

Comparison of the results of the present approach and the conventional methods is performed by first solving Equations (6) and (7) (conventional methods) as well as Equation (14) (proposed method) numerically for a given transmission line with geometrical and physical properties listed in Table 1, and then investigating the effects of these parameters on the response of the conductor.

4. 1. Standing or Travelling Wave The vibration amplitude of the transmission line with above mentioned properties in 25th mode is shown in Figure 6 (without damper) and Figure 7 (with one damper). In the damper-free case, there exist 24 nodes with zero amplitude along the span, but in the presence of the damper, the node with zero amplitude cannot be seen on the span. This means that the presence of damper converts the standing wave to travelling wave. The shape of vibration at near the damper and near the rigid support is similar to travelling wave and standing wave, respectively. Depiction of the vibrating conductor in successive times in Figure 8 shows these results more clearly. It is also observed that there is a kink (sudden change in conductor slope) in the conductor at the damper clamp which is associated with the concentrated damping and inertial forces exerted by the damper on the conductor. Experimental observations confirm the occurrence of this phenomenon [21, 29].

These Figures are obtained regardless of the effects of bending stiffness. In the real conductor (with bending stiffness), the slope change is not sudden in the damper point, but the rate of these changes, and as a result, the conductor curvature is very high. Since the increase in curvature, results in the increase of the bending stress which accelerates the fatigue failure, the probability of fatigue failure is very high in the location of clamps.

Since in the presented equations for the conductor response (Equation (14)), the effects of travelling wave, damper impedance, and the complex eigenvalue is considered in the vibration mode shape, the vibration response is different than a standing sinusoidal wave. For conductor with two dampers, the displacement amplitude of the dampers is calculated by two different methods (i.e. standing wave method and the new method) which are shown in Figure 9.

TABLE 1. Conductor properties

Cable type	D (mm)	ρ (kg/m)	T (kN)	EI (Nm^2)	L (m)
ACSR[2]	30	2	31	15	300

[2] Aluminum Conductor Steel Reinforced

Based on this Figure, the effect of the proposed parameters (wave travelling, damper impedance and complex eigenvalue) on the mode shape and vibration amplitude is not negligible. Therefore, given the significant effect of the damper amplitude on the dissipated energy and conductor amplitude, the calculation of the damper dissipated power based on simple sinusoidal mode shape is not an accurate method and will not yield valid results.

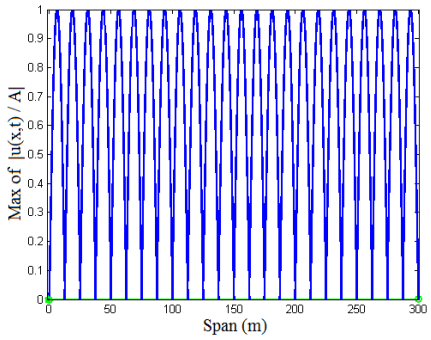

Figure 6. Distribution of the relative amplitude for the damper-free conductor along the span

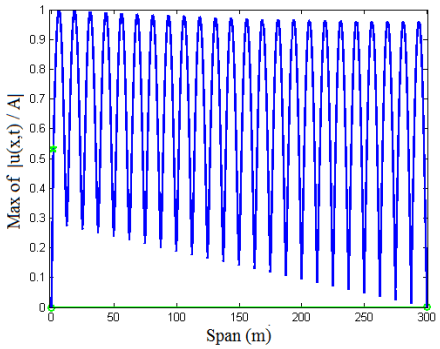

Figure 7. Distribution of the relative amplitude for the conductor with one damper at $x = 1.5\text{m}$

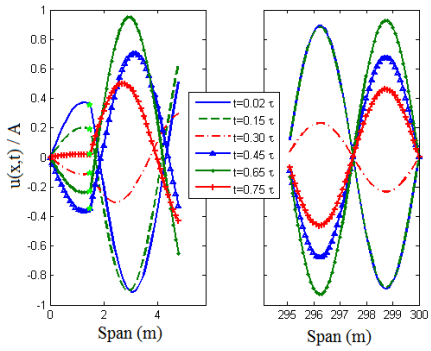

Figure 8. Standing wave in outer sub-span and travelling wave in inner sub-span for a conductor with one damper at $x = 1.5\text{m}$

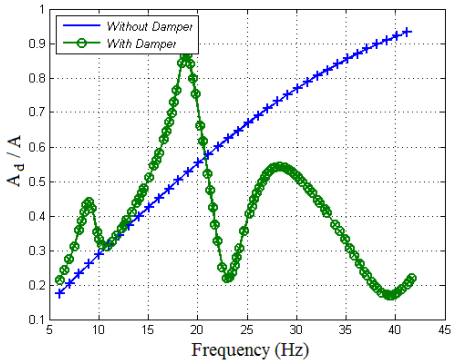

Figure 9. Effect of the damper impedance on the damper amplitude

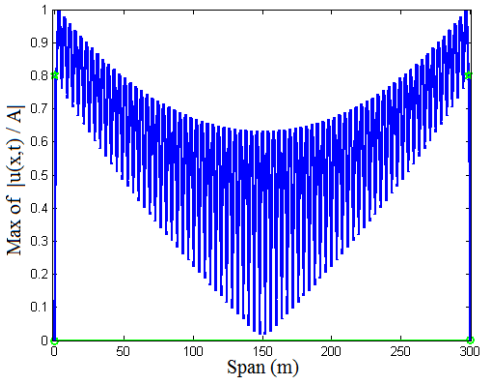

Figure 10. Distribution of the relative amplitude of the conductor with two dampers

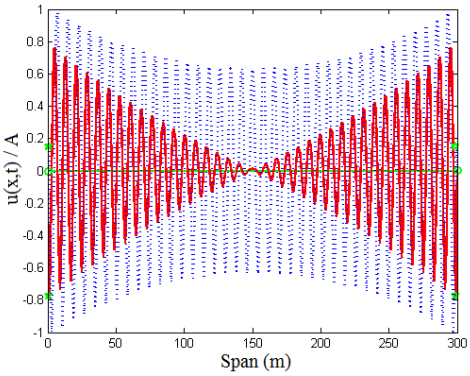

Figure 11. Vibration response at two different times for a conductor with two dampers

4. 2. Phase-amplitude Variations The relative amplitude distribution over the span for a conductor with two dampers at certain frequency is shown in Figure 10. According to this Figure, the amplitude of the adjacent points is significantly different. The depiction of the phase along the span also leads to a similar result. Figure 11 shows the conductor vibration at the same frequency in two different times and indicates the changes of the phase-amplitude of the conductor points with respect to time along the span. Variations of the amplitude and phase have a major effect on the calculation of curvature and bending stress of the conductor. Therefore, the results of conventional methods will not be adequately precise.

4. 3. Dissipated Power Variations The investigation of the similarity of the complex eigenvalues (Figure 12) with the damper amplitude (Figure 9) and damper dissipated power (Figure 13) shows that, the size of the real part of eigenvalue (damping rate) strongly influences the dissipated power of the dampers. The dissipated power in an eigenvalue which has a smaller damping rate is low whereas it is high in an eigenvalue with large damping rate. Thus, it is possible without the calculation of vibration amplitude and only through solving the eigenvalue problem, to determine the high-damping frequency bands (with high dissipation rate) and low-damping frequency bands (with low dissipation rate). Frequency bands with low dissipation rate, have high vibration potential. Based on Figure 12, frequency bands as 20-25 and 35-40 Hz are considered low damping areas and 15-20 and 25-30 Hz are high damping areas.

The obtained results by the new method for a condition in which two dampers are installed on the two sides of the span with the same distance from the support (symmetric locations) show that the dissipated power (Figure 13) and the damper amplitude, fully correspond with each other, and the sub-spans amplitudes are perfectly symmetrical.

When two dampers were installed at different distance from supports (asymmetric locations), the observed correspondence and symmetry disappears. Namely, the levels of dissipated energy in the dampers installed in different locations are significantly different from each other (Figure 14). This result violates the assumption of equality of dissipated energy of dampers that was taken for granted in the previous methods. The correspondence of the results in Figure 13 for the two dampers that are installed symmetrically is an indicator of the accuracy of the new presented method.

The results obtained by the proposed method for relative power dissipation of a conductor with different number of dampers are illustrated in Figure 15. This diagram shows dependency of dissipated power on number of dampers. The conventional method does not show this dependency. The relative dissipated power that obtained from Hagedorn method (Figure 4) does not change by installing three, four or five dampers on the conductor. Moreover, changes of power dissipation in Figure 4 is neither quantitatively nor qualitatively in accordance with Figure 15, whereas Figure 15 is in agreement with Figures 12 and 13.

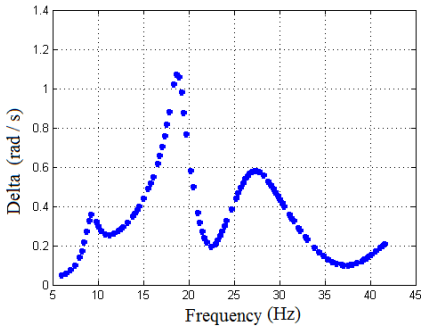

Figure 12. Complex eigenvalue of a conductor with two dampers at symmetric points

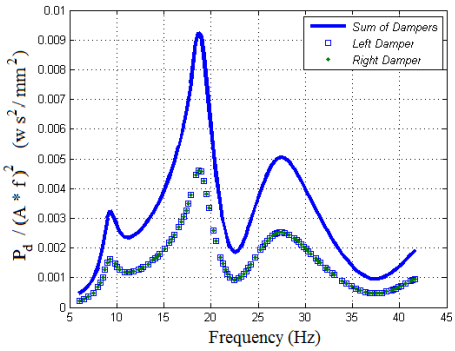

Figure 13. Relative power dissipation for a conductor with two dampers at symmetric points

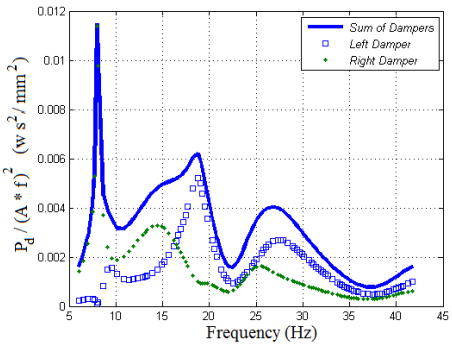

Figure 14. Relative power dissipation of a conductor with two dampers at asymmetric points

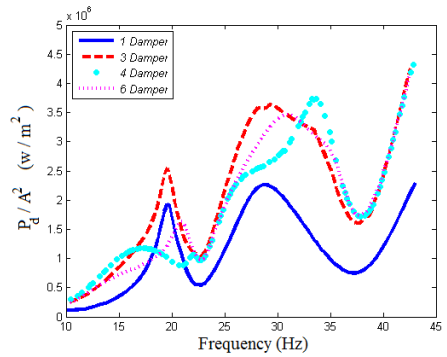

Figure 15. Change of relative dissipation power of a conductor with different number of dampers

5. CONCLUSION

This article presented a comprehensive model for conductor with arbitrary number of dampers. With this model, one can calculate the vibration response of a conductor with several dampers as well as the dissipated power of each damper with more precision. The current method considers the effect of wave travelling, damper location and damper impedance, as well as the effect of finite length of conductor and the phase-amplitude variations on conductor mode shapes and damper dissipated power. Such factors have significant impact on the accuracy of the responses but were overlooked in conventional methods. In addition to confirming the formation of standing wave in damper-free state, the obtained results of the present paper also indicate that in the presence of a damper in the inner sub-spans the wave travels and propagates towards the dampers.

Results of this study show that, complex eigenvalues, in addition to dynamic characteristics of the damper, are a function of dampers installation point and the real part of eigenvalues (which is ignored in other methods) is an important parameter in determining the energy dissipation of the dampers. Using this parameter, the frequency bands of high vibration potential can be identified without the need to extract the vibration amplitude.

6. REFERENCES

1. Kiessling, F., Nefzger, P., Kaintzyk, U. and Nolasco, J.F., "Overhead power lines: Planning, design, construction, Springer Science & Business Media, (2003).
2. Chan, J., Havard, D., Rawlins, C., Diana, G., Cloutier, L., Lilien, J.-L., Hardy, C., Wang, J. and Goel, A., "Epri transmission line reference book: Wind-induced conductor motion", (2009).
3. Bayliss, C., Bayliss, C.R. and Hardy, B.J., "Transmission and distribution electrical engineering, Elsevier, (2012).
4. und Kern, H., "Wind-induced vibrations on high-voltage overhead lines", ***Surv. Math. Ind***, Vol. 1, No., (1991), 145.
5. Emamgholizadeh, M., Gharabaghi, A.M., Abedi, K. and Sedaaghi, M., "Experimental investigation of the effect of splitter plate angle on the under-scouring of submarine pipeline due to steady current and clear water condition", ***International Journal of Engineering-Transactions C: Aspects***, Vol. 28, No. 3, (2014), 368.
6. Golafshani, A. and Gholizad, A., "Passive vibration control for fatigue damage mitigation in steel jacket platforms", ***International Journal of Engineering-Transactions B: Applications***, Vol. 21, No. 4, (2008), 313.
7. Dulhunty, P., "Vibration dampers on aac and aaac conductors", Vol., No., (2013).
8. Varney, T., "Notes on the vibration of transmission-line conductors", ***AIEE, Journal of the***, Vol. 45, No. 10, (1926), 953-957.
9. Claren, R. and Diana, G., "Mathematical analysis of transmission line vibration", ***IEEE Transactions on power***

Apparatus and Systems, Vol. 12, No. PAS-88, (1969), 1741-1771.

10. Langlois, S. and Legeron, F., "Prediction of aeolian vibration on transmission-line conductors using a nonlinear time history model—part i: Damper model", ***Power Delivery, IEEE Transactions on***, Vol. 29, No. 3, (2014), 1168-1175.
11. Godard, B., Guérard, S. and Lilien, J.-L., "Original real-time observations of aeolian vibrations on power-line conductors", ***IEEE Transactions on Power Delivery***, Vol. 26, No. 4, (2011), 2111-2117.
12. LI, L., KONG, D.-y., LONG, X.-h. and LIANG, Z.-p., "Analysis of aeolian transmission conductor with dampers by the finite element method [j]", ***High Voltage Engineering***, Vol. 2, (2008), 026.
13. Krispin, H., Fuchs, S. and Hagedorn, P., "Optimization of the efficiency of aeolian vibration dampers", in Power Engineering Society Conference and Exposition in Africa, 2007. PowerAfrica'07. IEEE, IEEE., (2007), 1-3.
14. Dhotarad, M., Ganesan, N. and Rao, B., "Transmission line vibrations", ***Journal of Sound and Vibration***, Vol. 60, No. 2, (1978), 217-237.
15. Hagedorn, P., "Ein einfaches rechenmodell zur berechnung winderregter schwingungen an hochspannungsleitungen mit dämpfern", ***Ingenieur-Archiv***, Vol. 49, No. 3-4, (1980), 161-177.
16. Hagedorn, P., "On the computation of damped wind-excited vibrations of overhead transmission lines", ***Journal of Sound and Vibration***, Vol. 83, No. 2, (1982), 253-271.
17. Wolf, H., Adum, B., Semenski, D. and Pustaić, D., "Using the energy balance method in estimation of overhead transmission line aeolian vibrations", ***Strojarstvo: časopis za teoriju i praksu u strojarstvu***, Vol. 50, No. 5, (2008), 269-276.
18. KASAP, H., "Investigation of stockbridge dampers for vibration control of overhead transmission lines", Middle East Technical University, (2012),
19. Sadeghi, M. and Rezaei, A., "Extending energy balance method for calculating cable vibration with arbitrary number of dampers and their optimal placement", ***Modares Mechanical Engineering***, Vol. 15, No. 8, (2015), 438-448.
20. Vecchiarelli, J., "Aeolian vibration of a conductor with a stockbridge-type damper", (1997).
21. Vecchiarelli, J., Currie, I. and Havard, D., "Computational analysis of aeolian conductor vibration with a stockbridge-type damper", ***Journal of Fluids and Structures***, Vol. 14, No. 4, (2000), 489-509.
22. Korayem, M. and Alipour, A., "Dynamic analysis of moving cables with variable tension and variable speed", (2010).
23. Langlois, S., Legeron, F. and Levesque, F., "Time history modeling of vibrations on overhead conductors with variable bending stiffness", ***Power Delivery, IEEE Transactions on***, Vol. 29, No. 2, (2014), 607-614.
24. Levesque, F., Goudreau, S., Langlois, S. and Legeron, F., "Experimental study of dynamic bending stiffness of acsr overhead conductors".
25. Braga, G., Nakamura, R. and Furtado, T., "Aeolian vibration of overhead transmission line cables: Endurance limits", in Transmission and Distribution Conference and Exposition: Latin America, IEEE/PES, IEEE., (2004), 487-492.
26. Hagedorn, P., "Wind-excited vibrations of transmission lines: A comparison of different mathematical models", ***Mathematical Modelling***, Vol. 8, (1987), 352-358.
27. Guérard, S., "Power line conductors, a contribution to the analysis of their dynamic behaviour", (2011).
28. Eskandari, G.M. and Nourzad, A., "Wave equations in transversely isotropic media in terms of potential functions", (2003).
29. IEEE Standards, "Ieee std. 563- ieee guide on conductor self damping measurements", in IEEE Power & Energy Society, New York, U. S. A., (1978 of Conference).
30. Noiseux, D., "Similarity laws of the internal damping of stranded cables in transverse vibrations", ***Power Delivery, IEEE Transactions on***, Vol. 7, No. 3, (1992), 1574-1581.
31. IEC Standards, "Iec std 61897- requirements and tests for stockbridge type aeolian vibration dampers", in International Electro technical Commission, Switzerland., (1998 of Conference).
32. Achenbach, J., "Wave propagation in elastic solids, Elsevier, (2012).

Aeolian Vibrations of Transmission Line Conductors with More than One Damper

A. Rezaei, M. H. Sadeghi

Mechanical Engineering Department, University of Tabriz, Tabriz, Iran

P A P E R I N F O

Paper history:
Received 23 June 2015
Received in revised form 01 September 2015
Accepted 03 September 2015

Keywords:
Aeolian Vibration
Transmission Line
Stock–bridge Damper
Energy Dissipation

چکیده

برای کاهش خسارات ارتعاشات «آولین» رساناهای خطوط انتقال برق به شبکه‌های انتقال توان الکتریکی، رایج‌ترین روش استفاده از میراگر «استاک‌بریج» است. برآورد انرژی اتلافی میراگر که فاکتور مهمی در تعیین تعداد و محل نصب میراگرهاست، به شدت به شکل مود فرض شده برای ارتعاش رسانا وابسته است. نتایج تحقیق حاضر نشان می‌دهد، روش‌های موجود نمی-توانند جواب دقیقی برای انرژی اتلافی رسانای دارای بیش از یک میراگر ارایه دهند. در این تحقیق روش جامعی برای محاسبه‌ی شکل مود و انرژی اتلافی میراگرهای متعدد نصب شده روی رسانا ارایه می‌شود که اثرات روندگی موج، تغییرات دامنه و فاز، شرایط مرزی دو انتها و همچنین تاثیر تعداد، محل نصب و امپدانس میراگر را در شکل مود ارتعاشی لحاظ می‌کند. همچنین با استفاده از این روش، می‌توان نواحی فرکانسی با پتانسیل ارتعاش بالا را بدون نیاز به محاسبه دامنه ارتعاش، شناسایی کرد.

***doi**:10.5829/idosi.ije.2015.28.10a.16*